Inorg. Chem. **1981**, *20*, 1038–1046

Contribution from the Department of Chemistry, University of Colorado, Boulder, Colorado 80309,
and the School of Chemical Sciences, University of Illinois, Urbana, Illinois 61801

Weak Magnetic Exchange Interactions between Paramagnetic Metal Ions and Coordinated *o*-Semiquinones in M(9,10-phenanthrenesemiquinone)$_2$(pyridine)$_2$ [M = Nickel(II) and Cobalt(II)] and Tetranuclear M$_4$(*o*-semiquinone)$_8$ Complexes

MICHAEL W. LYNCH,[1] ROBERT M. BUCHANAN,[2] CORTLANDT G. PIERPONT,*[2]
and DAVID N. HENDRICKSON*[1]

Received June 16, 1980

The X-ray structure of Ni(phenSQ)$_2$(py)$_2$·py, where phenSQ is the monoanion semiquinone of 9,10-phenanthrenequinone and py is pyridine, has been determined on a Syntex P$\bar{1}$ computer-automated diffractometer. Some 1622 unique reflections were used in the refinement to give final discrepancy indices of $R_F = 0.063$ and $R_{wF} = 0.065$. The complex crystallizes in the monoclinic space group $P2_1/c$ in a cell having the dimensions of $a = 12.364$ (4) Å, $b = 23.215$ (5) Å, $c = 12.475$ (4) Å, and $\beta = 109.97$ (2)°. The observed and calculated densities are 1.41 (1) and 1.406 g cm^{-3}, respectively. One pyridine molecule is present as a noninteracting solvate in Ni(phenSQ)$_2$(py)$_2$·py. The other two pyridines are coordinated in a cis fashion and together with the two chelating *o*-semiquinone ligands provide for a pseudooctahedral coordination geometry about the nickel ion. The two quinone-derived ligands have bond dimensions that are in keeping with an *o*-semiquinone formulation. The nickel–ligand atom distances indicate that the nickel ion is divalent. In the solid state there is a pairwise association to give [Ni(phenSQ)$_2$(py)$_2$]$_2$ units as a result of a π–π interaction of two phenSQ ligands coordinated to different nickel(II) ions. Variable-temperature (4.2–286 K) magnetic susceptibility data for Ni(phenSQ)$_2$(py)$_2$ and the analogous Ni(3,5-DBSQ)$_2$(bpy) (3,5-DBSQ is the semiquinone of 3,5-di-*tert*-butyl-1,2-benzoquinone and bpy is 2,2′-bipyridine) and Co(phenSQ)$_2$(py)$_2$ complexes clearly show that the quinone-derived ligands are, in fact, *o*-semiquinones and that the *intra*molecular antiferromagnetic exchange interaction between coordinated *o*-semiquinone ligand and paramagnetic metal ion is weak in these complexes. Magnetic susceptibility data are also presented for the tetranuclear complexes Ni$_4$(3,5-DBSQ)$_8$, Ni$_4$(phenSQ)$_8$, Co$_4$(3,5-DBSQ)$_8$, and Co$_4$(3,5-DBSQ)$_8$, and the same two observations are made about the ligand nature and *intra*molecular exchange. Theoretical equations are given to assess the magnetic exchange parameters for these two types of complexes as well as for the tris(*o*-semiquinone) complexes of iron(III) and chromium(III). The magnitude of *intra*molecular antiferromagnetic exchange interaction between metal ion and *o*-semiquinone ligand is found to vary in the order Cr(III) > Fe(III) > Co(II) > Ni(II). An explanation is advanced for this trend in terms of molecular orbitals.

Introduction

Transition-metal complexes with ligands derived from quinones are of interest not only because the metal ions in such complexes are redox active but also because the quinone-derived ligands can be redox active.[3] Complexes where the quinone-derived ligands are π bonding[4,5] and where they are σ bonding[6-8] have been reported. Quinone-derived ligands can potentially bond to metal ions in three oxidation states: quinone, semiquinone, or hydroquinone. In the case of *o*-quinones, the semiquinone form can be stabilized by chelation to a metal ion. An EPR investigation of *o*-semiquinone complexes of diamagnetic metal ions appeared in 1964.[9] A number of semiquinone complexes of low-spin cobalt(III) have been prepared and studied with EPR, IR, and UV–visible electronic absorption spectroscopies.[10-13]

o-Semiquinone complexes of paramagnetic transition-metal ions have recently been characterized. The compound Fe$^{\mathrm{II}}$(salen), where salen is the dianion of *N*,*N*′-ethylenebis(salicylidenimine), has been shown to oxidatively add *o*-quinones to give Fe$^{\mathrm{III}}$(salen)(*o*-SQ), where *o*-SQ can be the semiquinone form of 1,2-naphthoquinone, 9,10-phenanthrenequinone, or 3,5-di-*tert*-butyl-1,2-benzoquinone. There is a relatively strong antiferromagnetic exchange interaction between the semiquinone ligand ($S = {}^1/_2$) and the high-spin iron(III) ion ($S = {}^5/_2$) as documented by ^{57}Fe Mössbauer, magnetic susceptibility, and IR results. Three tris(*o*-semiquinone) complexes of high-spin iron(III) have also been prepared.[14,15] One of these complexes behaves as an $S = 1$ complex at room temperature with two unpaired electrons in the ground state and no appreciable thermal population in any excited state. The other two of these complexes have values of μ_{eff}/Fe at room temperature that are in excess of simple $S = 1$ complexes, and it was suggested that the *intra*molecular magnetic exchange interaction is only moderately strong in these two complexes. The analogous tris(*o*-semiquinone) complexes of chromium(III), Cr(*o*-SQ)$_3$, were also shown to have temperature-dependent μ_{eff} values.[14,15] As in the case of the iron analogue,[14] the Cr(3,5-DBSQ)$_3$ complex was found to have a relatively strong interaction between the *o*-semiquinone ligand and the Cr(III) ion such that the complex is diamagnetic at room temperature, indicating no significant population of spin states above the $S = 0$ ground state.[16] A molecular orbital diagram was used to show that it is reasonable to view the neutral tris coordinated complexes as tris(*o*-semiquinone) complexes of chromium(III).[17]

In the present paper the results of a study of complexes which could be formulated as semiquinone complexes of either

---

(1) University of Illinois.
(2) University of Colorado.
(3) (a) Becker, H. O. In "The Chemistry of Quinoid Compounds"; Patai, S., Ed.; Part 2, Chapter 7. (b) Foster, R.; Foreman, M. I. *Ibid.* Chapter 6.
(4) Uchtman, U. S.; Dahl, L. F. *J. Organomet. Chem.* **1972**, *40*, 403.
(5) Bodner, G. M.; Englemann, T. R. *J. Organomet. Chem.* **1975**, *88*, 391.
(6) Röhrscheid, F.; Balch, A. L.; Holm, R. H. *Inorg. Chem.* **1966**, *5*, 1542.
(7) Cenini, S.; Ugo, R.; LaMonica, G. *J. Chem. Soc. A* **1971**, 416.
(8) (a) Pierpont, C. G.; Francesconi, L. C.; Hendrickson, D. N. *Inorg. Chem.* **1978**, *17*, 3470. (b) Pierpont, C. G.; Francesconi, L. C.; Hendrickson, D. N. *Ibid.* **1977**, *16*, 2367 and references therein.
(9) Eaton, D. R. *Inorg. Chem.* **1964**, *3*, 1268.
(10) Kessel, S. L.; Emberson, R. M.; Debrunner, P. G.; Hendrickson, D. N. *Inorg. Chem.* **1980**, *19*, 1170.
(11) VonZelewsky, A.; Haas, O. *Proc. Int. Conf. Coord. Chem., 16th* **1974**, 2.25b.
(12) Wicklund, P. A.; Beckmann, L. S.; Brown, D. G. *Inorg. Chem.* **1976**, *15*, 1996.
(13) Brown, D. G.; Hemphill, W. D. *Inorg. Chem.* **1979**, *18*, 2039.
(14) Buchanan, R. M.; Kessel, S. L.; Downs, H. H.; Pierpont, C. G.; Hendrickson, D. N. *J. Am. Chem. Soc.* **1978**, *100*, 7894.
(15) Buchanan, R. M.; Down, H. H.; Shorthill, W. B.; Pierpont, C. G.; Kessel, S. L.; Hendrickson, D. N. *J. Am. Chem. Soc.* **1978**, *100*, 4318.
(16) Sofen, S. R.; Ware, D. C.; Cooper, S. R.; Raymond, K. N. *Inorg. Chem.* **1979**, *18*, 234.
(17) Downs, H. H.; Buchanan, R. M.; Pierpont, C. G. *Inorg. Chem.* **1979**, *18*, 1736.

0020-1669/81/1320-1038$01.25/0

Table I. Crystallographic Data for Ni(9,10-phenSQ)$_2$(NC$_5$H$_5$)$_2$·NC$_5$H$_5$

fw = 712.41	d(calcd) = 1.406 g cm^{-3}
monoclinic	d(exptl) = 1.41 (1) g cm^{-3}
space group: $P2_1/c$	$Z = 4$
a = 12.364 (4) Å	μ = 6.30 cm^{-1}
b = 23.215 (5) Å	scan rate: 4°/min
c = 12.475 (4) Å	2θ limits: $3° \leq 40°$
β = 109.97 (2)°	scan range: ±0.7°
V = 3365 (2) Å^3	data measd: 3556
Mo Kα (λ 0.710 73 Å)	data $F_o^2 > 3\sigma(F_o^2)$: 1622

nickel(II) or cobalt(II) are presented. The X-ray structure of the bis(3,5-di-*tert*-butyl-1,2-benzosemiquinone)cobalt(II) tetramer, Co$_4$(3,5-DBSQ)$_8$, was just recently reported,[18] and in this paper the X-ray structure of mononuclear Ni(phenSQ)$_2$(py)$_2$·py, where phenSQ is the 9,10-phenanthrenesemiquinone monoanion and py is pyridine, is described. Magnetic susceptibility data in the range of 4.2–286 K are presented for three mononuclear complexes, Ni(phenSQ)$_2$(py)$_2$, Co(phenSQ)$_2$(py)$_2$, and Ni(3,5-DBSQ)$_2$(bpy), and for four tetranuclear complexes, Co$_4$(3,5-DBSQ)$_8$, Co$_4$(phenSQ)$_8$, Ni$_4$(3,5-DBSQ)$_8$, and Ni$_4$(phenSQ)$_8$. These nickel(II) and cobalt(II) complexes were judiciously selected to demonstrate that weak antiferromagnetic exchange interactions can exist between paramagnetic metal ions and coordinated *o*-semiquinones.

Experimental Section

Magnetic Susceptibility. Variable-temperature (4.2–286 K) magnetic susceptibility data were obtained with a PAR Model 150A vibrating-sample magnetometer. A calibrated GaAs diode was used to monitor the sample temperature. A CuSO$_4$·5H$_2$O standard was also used. The data were least-squares fit with an adapted version of the function minimization program known as STEPT.[19]

Compound Preparation. Preparative procedures for the complexes used in this investigation have appeared previously. We have reported the synthesis of [Co(3,5-DBSQ)$_2$]$_4$ and Co(3,5-DBSQ)(3,5-DBCat)(bpy).[20] The 9,10-phenanthrenesemiquinone complexes M(phenSQ)$_2$ and M(phenSQ)$_2$(py)$_2$, where M = Ni or Co, were prepared by the procedures published by Floriani and Calderazzo.[21] In our hands the pyridine adducts are obtained as pyridine solvates.

Structure Determination of Ni(O$_2$C$_{14}$H$_8$)$_2$(NC$_5$H$_5$)$_2$·NC$_5$H$_5$. Preliminary photographs taken on a crystal obtained directly from a pyridine solution indicated monoclinic symmetry. Systematic absences were consistent with space group $P2_1/c$. A crystal of dimensions 0.28 × 0.29 × 0.38 mm was mounted and centered on a Syntex P$\bar{1}$ automated diffractometer equipped with a graphite-crystal monochromator. The centered settings of 15 reflections were used to calculate the cell constants given in Table I. Data were collected at ambient room temperature over the angular range $3° \leq 2\theta \leq 40°$. A decline of 10% was observed for the intensities of standard reflections during the time required for data collection. Corrections were applied for this decrease during data processing. As we have found throughout our structural work on quinone complexes, crystals of Ni(O$_2$C$_{14}$H$_8$)$_2$(NC$_5$H$_5$)$_2$·NC$_5$H$_5$ diffracted very weakly. In this particular case it may be related to disorder of the nitrogen of the pyridine solvate molecule. The free pyridine molecule was found to be well separated from the complex molecule with no strong intermolecular forces of the type found previously in benzene solvates. Consequently, the solvent is easily displaced from the lattice, accounting for the decay in the intensity of standard reflections during data collection. With the relatively large thermal parameters associated with the atoms of the pyridine solvate it would be difficult to differentiate an ordered nitrogen atom from an atom which is one-sixth nitrogen and five-sixths carbon. The assignment of N(3) in Table II was based on the observation that its isotropic thermal parameter, in cycles where all six atoms were assigned carbon scattering factors, was slightly lower than the other five atoms. Interatomic distances within the solvate are essentially the same. Of the 3556 reflections measured only 1622 were found to have $F_o^2 > 3\sigma(F_o^2)$ and were included in the refinement.

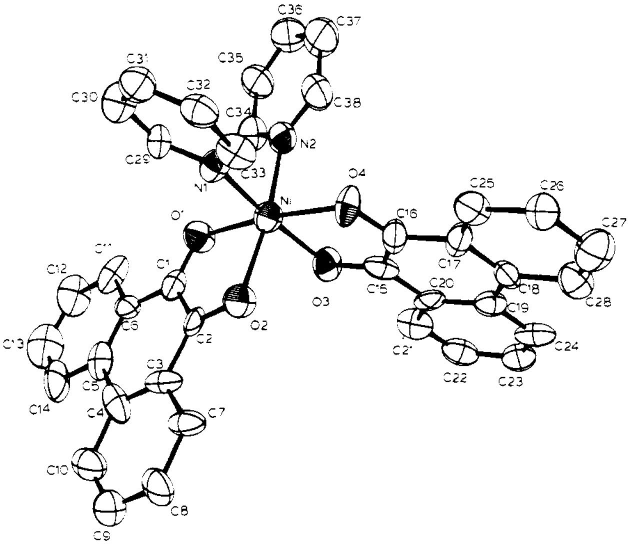

Figure 1. ORTEP plot of Ni(phenSQ)$_2$(py)$_2$. Hydrogen atoms are not shown.

The structure was solved by using MULTAN-78 and refined by using procedures and programs described previously.[22] The final cycle of refinement converged with $R_F = 0.063$ and $R_{wF} = 0.065$. The standard deviation of an observation of unit weight was 1.42. Final positional and thermal parameters and their estimated standard deviations are listed in Table II. Values for F_o and F_c (×10) are available as supplementary material.

Results and Discussion

Structural Features of Ni(phenSQ)$_2$(py)$_2$·py. The X-ray structure of Ni(phenSQ)$_2$(py)$_2$·py was solved by standard heavy-atom techniques. One pyridine molecule is not coordinated to the nickel ion and is found as a noninteracting solvate molecule. A view of the Ni(phenSQ)$_2$(py)$_2$ molecule is shown in Figure 1. A comparison of powder diffraction data on this complex with its cobalt analogue suggest that the two complexes are isostructural. Intramolecular bond lengths and angles are given in Table III.

The complex molecule has a cis structure with Ni–O and Ni–N lengths which are typical of Ni(II). Trans quinone oxygen atoms O(1) and O(4) have equivalent Ni–O lengths of 2.022 (7) and 2.028 (7) Å. These values compare well with a value of 2.024 (4) Å reported for *trans*-bis(2,4-pentanedionato)bis(pyridine)nickel(II)[23] and 2.021 (4) Å for the trans Ni–O lengths of the acetylacetonate ligands in *cis*-bis(2,4-pentanedionato)bis(pyridine *N*-oxide)nickel(II).[24] In Ni(phenSQ)$_2$(py)$_2$ the Ni–O lengths for the quinone oxygen atoms trans to pyridine nitrogen donors are slightly longer (2.082 (7) and 2.100 (7) Å), reflecting the trans influence of the pyridine ligands. Nickel–nitrogen lengths to the pyridine ligands of 2.069 (9) and 2.099 (9) Å also agree with other Ni(II) values. The Ni–N length of *trans*-Ni(acac)$_2$(py)$_2$ is 2.112 (5) Å. Since the ionic radii of divalent nickel and cobalt ions are quite similar it is useful to compare the Ni–O lengths of this complex with the values found for the bis(3,5-di-*tert*-butyl-semiquinone)cobalt(II) tetramer.[18] The average Co–O length of 2.05 (2) Å found in this structure is in close

---

(18) Buchanan, R. M.; Fitzgerald, B. J.; Pierpont, C. G. *Inorg. Chem.* **1979**, *18*, 3439.

(19) Chandler, J. P. Program 66, Quantum Chemistry Program Exchange, Indiana University, Bloomington, Ind.

(20) Buchanan, R. M.; Pierpont, C. G. *J. Am. Chem. Soc.* **1980**, *102*, 4951.

(21) Floriani, C.; Henzi, R.; Calderazzo, F. *J. Chem. Soc., Dalton Trans.* **1972**, 2640.

(22) Pierpont, C. G. *Inorg. Chem.* **1977**, *16*, 363.

(23) Elder, R. C. *Inorg. Chem.* **1968**, *7*, 2316.

(24) Horrocks, W. D.; Templeton, D. H.; Zalkin, A. *Inorg. Chem.* **1968**, *7*, 1552.

(25) Pierpont, C. G.; Buchanan, R. M. *J. Am. Chem. Soc.* **1975**, *97*, 6450.

Table II. Positional and Thermal Parameters for the Atoms of $Ni(O_2C_{14}H_8)_2(NC_5H_5)_2{\cdot}NC_5H_5$

atom	*x*	*y*	*z*	B_{11}[a]	B_{22}	B_{33}	B_{12}	B_{13}	B_{23}
Ni	0.05835 (15)	0.06279 (7)	0.30763 (12)	3.9 (1)	4.2 (1)	2.9 (1)	0.2 (1)	1.4 (1)	−0.2 (1)
O(1)	0.1549 (7)	0.0363 (3)	0.2142 (6)	4.6 (5)	5.1 (4)	3.7 (4)	0.9 (4)	1.9 (4)	0.4 (4)
O(2)	0.1828 (6)	0.0154 (3)	0.4313 (5)	3.9 (5)	5.4 (4)	3.5 (4)	0.3 (4)	2.0 (4)	0.2 (4)
C(1)	0.2385 (11)	0.0057 (5)	0.2730 (9)	3.8 (9)	3.7 (9)	3.3 (8)	−0.7 (8)	1.5 (7)	−1.1 (8)
C(2)	0.2549 (10)	−0.0051 (5)	0.3904 (9)	2.4 (8)	4.1 (9)	3.4 (7)	−0.1 (6)	0.9 (6)	−2.0 (6)
C(3)	0.3516 (10)	−0.0403 (5)	0.4560 (9)	2.0 (8)	4.1 (9)	3.6 (7)	−0.7 (6)	−0.5 (6)	0.1 (5)
C(4)	0.4319 (10)	−0.0623 (5)	0.4106 (10)	3.2 (8)	3.0 (6)	7.3 (9)	0.7 (8)	1.7 (8)	0.3 (8)
C(5)	0.4143 (10)	−0.0493 (5)	0.2889 (9)	3.9 (9)	2.9 (9)	4.9 (8)	−1.2 (6)	2.7 (7)	−0.6 (6)
C(6)	0.3216 (10)	−0.0162 (5)	0.2246 (9)	2.5 (8)	3.0 (9)	3.2 (8)	−0.7 (6)	0.0 (6)	−0.7 (6)
C(7)	0.3646 (10)	−0.0517 (5)	0.5738 (9)	4.0 (8)	2.4 (9)	4.3 (8)	−0.3 (6)	−1.1 (6)	−0.1 (6)
C(8)	0.4584 (12)	−0.0818 (5)	0.6396 (10)	5.2 (10)	4.1 (9)	5.0 (8)	0.8 (8)	0.2 (8)	−0.2 (6)
C(9)	0.5448 (12)	−0.1008 (6)	0.5936 (12)	4.1 (10)	5.2 (9)	6.9 (10)	1.8 (9)	−0.3 (8)	−0.6 (9)
C(10)	0.5280 (11)	−0.0925 (5)	0.4822 (11)	4.1 (9)	4.3 (9)	5.8 (8)	−0.1 (8)	1.5 (8)	−0.6 (8)
C(11)	0.3071 (11)	−0.0045 (5)	0.1103 (10)	6.4 (10)	3.0 (6)	4.7 (8)	−1.2 (8)	3.3 (8)	−1.0 (6)
C(12)	0.3904 (13)	−0.0239 (6)	0.0656 (11)	7.6 (12)	7.0 (11)	6.6 (10)	−1.2 (10)	6.0 (10)	−0.3 (9)
C(13)	0.4837 (13)	−0.0585 (7)	0.1299 (12)	6.8 (12)	7.0 (11)	9.0 (11)	−2.1 (11)	4.9 (10)	0.9 (11)
C(14)	0.4929 (11)	−0.0698 (5)	0.2390 (11)	4.1 (9)	4.8 (9)	6.9 (9)	1.0 (8)	3.1 (6)	−0.9 (9)
O(3)	0.1565 (7)	0.1380 (3)	0.3609 (6)	4.7 (5)	4.3 (4)	3.5 (4)	0.0 (4)	1.9 (4)	−0.2 (3)
O(4)	−0.0188 (7)	0.0943 (3)	0.4145 (5)	5.9 (6)	3.8 (4)	3.5 (4)	−0.3 (4)	3.0 (4)	−1.0 (4)
C(15)	0.1246 (9)	0.1638 (5)	0.4352 (8)	2.1 (7)	4.5 (9)	2.2 (6)	0.2 (6)	0.7 (5)	0.7 (5)
C(16)	0.0296 (11)	0.1407 (5)	0.4656 (9)	4.8 (9)	2.9 (9)	2.9 (6)	0.8 (8)	0.8 (6)	−0.6 (5)
C(17)	−0.0078 (10)	0.1672 (5)	0.5522 (8)	4.8 (8)	2.5 (6)	2.5 (6)	0.4 (6)	0.9 (6)	−1.0 (5)
C(18)	0.0497 (10)	0.2169 (5)	0.6067 (9)	3.0 (8)	4.3 (8)	3.1 (6)	1.6 (6)	1.1 (6)	0.5 (5)
C(19)	0.1435 (10)	0.2428 (5)	0.5761 (8)	3.4 (8)	4.0 (9)	2.0 (6)	0.2 (6)	0.2 (6)	0.0 (5)
C(20)	0.1815 (10)	0.2168 (5)	0.4903 (9)	3.1 (8)	4.5 (9)	1.9 (6)	0.3 (6)	−0.7 (6)	0.7 (5)
C(21)	0.2701 (11)	0.2405 (5)	0.4587 (10)	3.8 (9)	2.4 (9)	6.3 (9)	1.0 (6)	1.2 (8)	1.0 (6)
C(22)	0.3234 (11)	0.2911 (5)	0.5121 (10)	4.3 (9)	4.5 (9)	4.3 (8)	−0.6 (8)	1.1 (7)	1.0 (6)
C(23)	0.2887 (11)	0.3173 (5)	0.5946 (10)	5.8 (10)	4.1 (9)	3.7 (8)	−0.4 (8)	1.1 (7)	−0.1 (6)
C(24)	0.2032 (11)	0.2936 (6)	0.6258 (9)	3.2 (9)	5.6 (11)	4.0 (8)	0.4 (8)	1.1 (7)	1.3 (8)
C(25)	−0.0957 (11)	0.1411 (5)	0.5818 (9)	5.0 (9)	4.8 (9)	2.8 (6)	1.3 (6)	2.6 (6)	0.9 (5)
C(26)	−0.1260 (10)	0.1662 (6)	0.6668 (9)	3.0 (8)	6.1 (9)	4.0 (8)	−0.3 (8)	1.0 (6)	−0.8 (6)
C(27)	−0.0723 (11)	0.2169 (5)	0.7214 (9)	5.9 (10)	4.7 (9)	3.5 (7)	0.1 (8)	3.3 (8)	−0.6 (6)
C(28)	0.0140 (11)	0.2430 (5)	0.6918 (10)	4.1 (9)	3.1 (9)	5.1 (8)	−0.8 (6)	2.2 (6)	0.1 (6)
N(1)	−0.0482 (8)	−0.0086 (4)	0.2709 (7)	4.9 (7)	4.3 (6)	2.1 (5)	0.5 (5)	1.2 (5)	0.2 (4)
C(29)	−0.1121 (11)	−0.0235 (5)	0.3361 (8)	5.9 (10)	4.6 (9)	1.5 (6)	1.7 (8)	0.8 (6)	1.1 (6)
C(30)	−0.1878 (10)	−0.0700 (5)	0.3170 (9)	4.0 (9)	3.4 (9)	5.1 (8)	−0.3 (8)	1.6 (6)	0.4 (6)
C(31)	−0.1982 (11)	−0.1034 (5)	0.2231 (9)	4.6 (9)	4.5 (9)	3.8 (7)	1.1 (8)	0.2 (7)	−0.2 (6)
C(32)	−0.1333 (12)	−0.0886 (5)	0.1523 (9)	6.6 (9)	4.8 (8)	3.6 (9)	−1.6 (8)	2.7 (7)	−1.8 (6)
C(33)	−0.0608 (11)	−0.0424 (5)	0.1800 (9)	4.7 (9)	3.7 (9)	3.8 (8)	−0.1 (8)	1.4 (6)	−0.9 (6)
N(2)	−0.0582 (9)	0.1038 (4)	0.1647 (7)	4.8 (8)	2.9 (6)	4.8 (7)	0.8 (5)	1.7 (6)	0.1 (4)
C(34)	−0.1598 (12)	0.1202 (6)	0.1638 (9)	5.6 (10)	6.6 (11)	2.8 (8)	2.1 (9)	1.0 (8)	0.4 (6)
C(35)	−0.2421 (13)	0.1434 (6)	0.0688 (12)	6.5 (12)	6.5 (11)	6.1 (9)	−1.1 (10)	0.6 (10)	−0.2 (9)
C(36)	−0.2150 (14)	0.1480 (6)	−0.0296 (10)	9.2 (12)	7.9 (11)	3.2 (9)	4.1 (11)	−2.0 (10)	1.5 (9)
C(37)	−0.1094 (13)	0.1317 (6)	−0.0286 (10)	6.6 (12)	5.0 (9)	4.9 (10)	1.3 (9)	0.8 (9)	1.4 (8)
C(38)	−0.0281 (11)	0.1089 (5)	0.0716 (10)	5.3 (10)	5.3 (9)	4.0 (8)	−0.9 (8)	2.5 (8)	0.4 (8)
N(3)	−0.4654 (13)	0.2511 (6)	0.3923 (12)	8.8 (12)	9.5 (13)	11.6 (12)	0.8 (9)	4.9 (11)	−0.3 (10)
C(39)	−0.5085 (14)	0.2780 (6)	0.2973 (15)	7.7 (12)	6.1 (11)	8.5 (12)	−0.4 (9)	0.9 (11)	1.2 (10)
C(40)	−0.4563 (16)	0.2755 (7)	0.2112 (13)	8.3 (13)	7.8 (13)	6.7 (13)	0.6 (10)	−0.9 (10)	0.3 (10)
C(41)	−0.3574 (17)	0.2444 (7)	0.2334 (13)	13.5 (18)	7.8 (13)	5.6 (10)	−1.3 (11)	3.2 (11)	−1.1 (9)
C(42)	−0.3151 (13)	0.2150 (7)	0.3369 (15)	6.4 (11)	8.1 (11)	10.1 (12)	2.1 (9)	4.3 (11)	−0.1 (11)
C(43)	−0.3693 (16)	0.2201 (7)	0.4116 (12)	8.8 (14)	8.3 (13)	6.6 (10)	−1.1 (11)	3.2 (11)	−0.1 (9)

[a] The form of the anisotropic thermal ellipsoid is $\exp[-0.25(B_{11}h^2a^{*2} + B_{22}k^2b^{*2} + B_{33}l^2c^{*2} + 2B_{12}hka^*b^* + 2B_{13}hla^*c^* + 2B_{23}klb^*c^*)]$. The quantities given in the table are in units of A^2.

agreement with the Ni–O lengths of *cis*-Ni(phenSQ)$_2$(py)$_2$. This comparison is of interest because the bipyridine adduct of the cobalt tetramer has grossly different structural features. The Co–O and Co–N lengths of Co(3,5-DBCat)(3,5-DBSQ)(bpy) are typical of a Co(III) complex,[20] and an important point of interest in the present structure determination is the charge distribution within the complex molecule. This was reflected not only in the metal–ligand bond lengths in the cobalt case but also in the structural features of the quinone ligands. As we have pointed out previously, semiquinone ligands have C–O lengths of 1.29 (1) Å, while catecholate ligands have values of 1.35 (1) Å. This difference is present in Co(3,5-DBCat)(3,5-DBSQ)(bpy) but not in Ni(phenSQ)$_2$(py)$_2$. The average C–O length for the semiquinone ligands in *cis*-Ni(phenSQ)$_2$(py)$_2$ is 1.27 (1) Å. Other ligand-bonding parameters which are characteristic of semiquinone coordination are the carbon–carbon length between quinone carbon atoms and the ligand bite angle at the metal. For semiquinone ligands the C–C length is typically 1.44 (1) Å, and in the present case this value is 1.44 (1) Å. The ligand bite angle for catecholate ligands is typically 2° larger than the bite angle for chelated semiquinones. The value of 80.7 (3)° for the semiquinone ligands of Ni(phenSQ)$_2$(py)$_2$ agrees well with the value of 79.9 (2)° found for the chelated semiquinone ligands of [Co(3,5-DBSQ)$_2$]$_4$. The difference in charge distribution which we find for Ni(phenSQ)$_2$(py)$_2$ and its Co analogue relative to Co(3,5-DBCat)(3,5-DBSQ)(bpy) is significant and is further reflected in the magnetic properties of these complexes.

A feature of the crystal structure of Ni(phenSQ)$_2$(py)$_2$·py which might influence the magnetic properties in the solid state is the strong donor–acceptor stacking of ligands of adjacent molecules. Complex molecules exist in pairs within the unit cell, as shown in Figure 2. A crystallographic inversion center lies just below the plane of semiquinone ligand I. The interplanar separation between phenSQ ligands in 3.33 Å, a value which compares well with similar stacking found in the Fe(phenSQ)$_3$[15] and Mo$_2$O$_5$(phenSQ)$_2$[26] structures. This sep-

Table III. Bond Distances (Å) and Angles (Deg) for the *cis*-Ni(O$_2$C$_{14}$H$_8$)$_2$(NC$_5$H$_5$)$_2$ Complex Molecule

	Inner Coordination Sphere		
Ni–O(1)	2.028 (7)	Ni–O(4)	2.022 (7)
Ni–O(2)	2.082 (7)	Ni–N(1)	2.069 (9)
Ni–O(3)	2.100 (7)	Ni–N(2)	2.099 (9)
O(1)–Ni–O(2)	80.4 (3)	O(2)–Ni–O(4)	95.6 (3)
O(1)–Ni–N(1)	94.9 (3)	O(3)–Ni–O(4)	81.0 (3)
O(1)–Ni–N(2)	91.0 (3)	O(3)–Ni–N(1)	172.5 (3)
O(1)–Ni–O(3)	92.5 (3)	O(3)–Ni–N(2)	92.7 (3)
O(1)–Ni–O(4)	172.4 (3)	O(4)–Ni–N(1)	91.6 (3)
O(2)–Ni–O(3)	90.2 (3)	O(4)–Ni–N(2)	93.1 (3)
O(2)–Ni–N(1)	89.7 (3)	N(1)–Ni–N(2)	88.5 (3)
O(2)–Ni–N(2)	171.1 (3)		
	Semiquinone Ligand I		
C(1)–O(1)	1.262 (12)	C(7)–C(8)	1.374 (14)
C(2)–O(2)	1.262 (11)	C(8)–C(9)	1.443 (16)
C(1)–C(2)	1.429 (13)	C(9)–C(10)	1.347 (15)
C(2)–C(3)	1.448 (14)	C(10)–C(4)	1.406 (15)
C(3)–C(4)	1.397 (14)	C(11)–C(6)	1.402 (13)
C(4)–C(5)	1.489 (14)	C(11)–C(12)	1.402 (15)
C(5)–C(6)	1.385 (14)	C(12)–C(13)	1.410 (17)
C(1)–C(6)	1.450 (14)	C(13)–C(14)	1.352 (15)
C(3)–C(7)	1.443 (14)	C(14)–C(5)	1.405 (14)
Ni–O(1)–C(1)	111.2 (7)	C(6)–C(5)–C(14)	119.5 (11)
Ni–O(2)–C(2)	110.2 (7)	C(6)–C(5)–C(4)	120.4 (11)
O(1)–C(1)–C(6)	120.7 (10)	C(14)–C(5)–C(4)	120.1 (12)
O(1)–C(1)–C(2)	119.7 (11)	C(5)–C(6)–C(11)	119.3 (11)
C(2)–C(1)–C(6)	119.4 (11)	C(5)–C(6)–C(1)	121.2 (11)
O(2)–C(2)–C(1)	118.4 (11)	C(11)–C(6)–C(1)	119.5 (11)
O(2)–C(2)–C(3)	123.0 (10)	C(8)–C(7)–C(3)	118.3 (12)
C(1)–C(2)–C(3)	118.6 (11)	C(7)–C(8)–C(9)	120.7 (12)
C(4)–C(3)–C(7)	120.2 (11)	C(10)–C(9)–C(8)	119.5 (12)
C(4)–C(3)–C(2)	122.8 (11)	C(9)–C(10)–C(4)	121.7 (13)
C(7)–C(3)–C(2)	117.0 (17)	C(6)–C(11)–C(12)	119.1 (12)
C(3)–C(4)–C(10)	119.2 (12)	C(11)–C(12)–C(13)	121.8 (12)
C(3)–C(4)–C(5)	117.5 (11)	C(14)–C(13)–C(12)	116.9 (13)
C(10)–C(4)–C(5)	123.1 (12)	C(13)–C(14)–C(5)	123.3 (13)
	Semiquinone Ligand II		
O(3)–C(15)	1.275 (11)	C(21)–C(22)	1.399 (14)
O(4)–C(16)	1.290 (11)	C(22)–C(23)	1.384 (14)
C(15)–C(16)	1.454 (15)	C(23)–C(24)	1.361 (15)
C(16)–C(17)	1.450 (13)	C(24)–C(19)	1.417 (14)
C(17)–C(18)	1.402 (13)	C(25)–C(17)	1.399 (14)
C(18)–C(19)	1.468 (14)	C(25)–C(26)	1.370 (13)
C(19)–C(20)	1.439 (14)	C(26)–C(27)	1.370 (13)
C(20)–C(15)	1.468 (14)	C(27)–C(28)	1.382 (14)
C(20)–C(21)	1.398 (14)	C(28)–C(18)	1.417 (14)
Ni–O(3)–C(15)	109.4 (7)	C(28)–C(27)–C(26)	121.0 (11)
Ni–O(4)–C(16)	112.6 (8)	C(27)–C(26)–C(25)	121.4 (12)
C(3)–C(15)–C(16)	119.7 (11)	C(26)–C(25)–C(17)	117.6 (11)
O(3)–C(15)–C(20)	121.2 (11)	C(25)–C(17)–C(18)	122.6 (11)
O(4)–C(16)–C(15)	117.3 (10)	C(19)–C(20)–C(21)	122.1 (12)
O(4)–C(16)–C(17)	120.7 (12)	C(20)–C(21)–C(22)	118.8 (12)
C(15)–C(16)–C(17)	122.0 (11)	C(21)–C(22)–C(23)	120.6 (12)
C(16)–C(17)–C(18)	118.2 (12)	C(22)–C(23)–C(24)	120.2 (12)
C(17)–C(18)–C(19)	121.7 (11)	C(24)–C(19)–C(20)	114.9 (12)
C(18)–C(19)–C(20)	120.6 (11)	C(15)–C(20)–C(21)	119.6 (11)
C(19)–C(20)–C(15)	118.3 (12)	C(16)–C(17)–C(25)	119.1 (11)
C(20)–C(15)–C(16)	119.2 (11)	C(23)–C(24)–C(19)	123.4 (12)
C(17)–C(18)–C(28)	118.6 (11)	C(18)–C(19)–C(24)	124.5 (11)
C(18)–C(28)–C(27)	118.7 (11)	C(19)–C(18)–C(28)	119.7 (11)
	Pyridine Ligand I		
N(1)–C(29)	1.358 (13)	C(31)–C(32)	1.424 (15)
C(29)–C(30)	1.395 (15)	C(32)–C(33)	1.364 (14)
C(30)–C(31)	1.374 (14)	C(33)–N(1)	1.344 (12)
Ni–N(1)–C(29)	121.9 (8)	C(31)–C(30)–C(29)	116.4 (11)
Ni–N(1)–C(33)	122.4 (8)	C(30)–C(31)–C(32)	118.9 (12)
C(33)–N(1)–C(29)	115.7 (10)	C(33)–C(32)–C(31)	119.6 (11)
N(1)–C(29)–C(30)	126.0 (10)	C(32)–C(33)–N(1)	123.3 (12)
	Pyridine Ligand II		
N(2)–C(34)	1.309 (14)	C(36)–C(37)	1.356 (17)
C(34)–C(35)	1.341 (15)	C(37)–C(38)	1.412 (14)
C(35)–C(36)	1.383 (17)	C(38)–N(2)	1.341 (12)
Ni–N(2)–C(34)	121.2 (9)	C(34)–C(35)–C(36)	117.4 (14)
Ni–N(2)–C(38)	117.6 (9)	C(35)–C(36)–C(32)	119.7 (12)
C(34)–N(2)–C(38)	121.1 (10)	C(36)–C(37)–C(38)	120.3 (13)
N(2)–C(34)–C(35)	123.0 (12)	C(37)–C(38)–N(2)	118.4 (12)

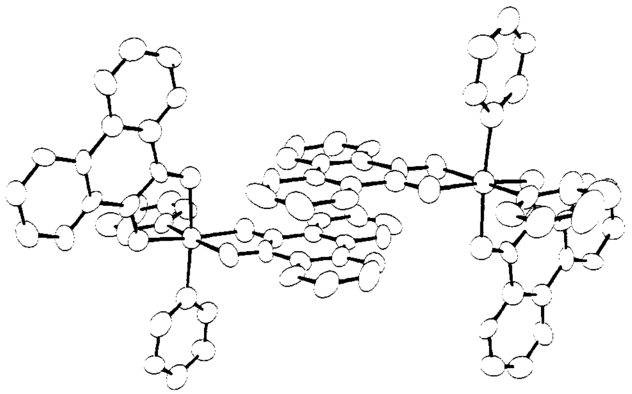

Figure 2. ORTEP plot showing dimeric association of Ni(phenSQ)$_2$(py)$_2$ in the solid state.

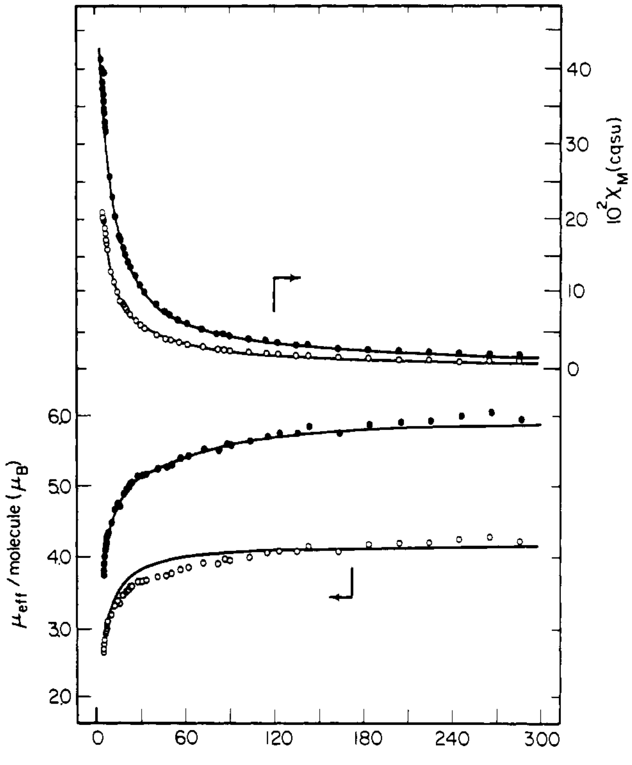

Figure 3. Effective magnetic moment and molar paramagnetic susceptibility vs. temperature curves for Ni(phenSQ)$_2$(py)$_2$. The data are plotted in two different ways. In one case (○) the μ_{eff} and χ_M vaues are given per Ni(phenSQ)$_2$(py)$_2$ unit, whereas in the other case (●) the data are given per dimer [Ni(phenSQ)$_2$(py)$_2$]$_2$. The solid lines represent least-squares fits to two different models; see text.

aration is relatively short for aromatic systems and reflects a strong interaction. The pyridine solvate in the crystal structure is well separated from the complex molecule and not involved with donor–acceptor pairing. This accounts for the facility with which the solvent is displaced leading to crystal decomposition.

Magnetism of Mononuclear Complexes. Magnetic susceptibilities were determined for Ni(phenSQ)$_2$(py)$_2$, Ni(3,5-DBSQ)$_2$(bpy), and Co(phenSQ)$_2$(py)$_2$. The data are given in Tables IV–VIII,[26] respectively. Figure 3 illustrates the data obtained for Ni(phenSQ)$_2$(py)$_2$ (the pyridine solvate molecule is lost before the measurements are made), where it can be seen that only below ca. 30 K is there an appreciable reduction in the effective magnetic moment. The value of μ_{eff} per

---

[26] Supplementary material.

Table IX. Effective Magnetic Moments

compd	μ_{eff}/molecule, μ_B 286 K	μ_{eff}/molecule, μ_B 4.2 K	μ_{eff}/$M(SQ)_2$ unit, μ_B 286 K
$Co(phenSQ)_2(py)_2$	5.43	1.78	5.43
$Ni(phenSQ)_2(py)_2$	4.20	2.62	4.20
$Ni(3,5\text{-}DBSQ)_2(bpy)$	4.30	3.90	4.30
$Co_4(3,5\text{-}DBSQ)_8$	9.16[a]	4.63	4.58
$Co_4(phenSQ)_8$	9.18[a]	7.16	4.59
$Ni_4(3,5\text{-}DBSQ)_8$	8.69	5.73	4.35
$Ni_4(phenSQ)_8$	6.32	3.24	3.16

[a] Actual temperature is 224 K.

molecule of $Ni(phenSQ)_2(py)_2$ is 4.20 μ_B at 286 K, as summarized in Table IX. This is very informative because it is only explicable in terms of an $S = 1$ nickel(II) ion coordinated by two $S = {}^1/_2$ semiquinone ligands with a *weak magnetic exchange interaction* between them. The complex would be diamagnetic if it consisted of nickel(0) coordinated by two quinone ligands, and nickel(III)–semiquinone–catecholate and $Ni^{IV}(catecholate)_2$ formulations are improbable. With no *intra*molecular magnetic exchange interaction, a complex with an $S = 1$ metal and two $S = {}^1/_2$ ligands should have a spin-only μ_{eff} value of 3.74 μ_B per complex. The observed value of 4.20 μ_B at 286 K exceeds the spin-only value, of course, because pseudooctahedral nickel(II) ions will generally give μ_{eff} values in excess of the spin-only value.

It is of interest to determine the magnitude of the *intra*molecular magnetic exchange interaction present in $Ni(phenSQ)_2(py)_2$; however this goal is made difficult by virtue of the intermolecular interactions present in the solid. As indicated above, the $Ni(phenSQ)_2(py)_2$ molecules are associated in pairs in the solid state, wherein a phenSQ ligand from one complex is involved in an apparently strong π–π interaction with one phenSQ ligand of a second complex. Two different theoretical models were used to fit the susceptibility data and, more particularly, the attenuation in μ_{eff} seen below ca. 30 K. In the case of model 1, it was assumed that the (π–π) phenSQ–phenSQ interaction is negligible and that the intramolecular interactions in $Ni(phenSQ)_2(py)_2$ could be analyzed with two exchange parameters as schematically indicated by

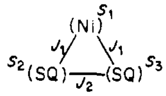

Each pairwise exchange interaction is assumed to be isotropic and of the standard form $\hat{H} = -2J\hat{S}_i\cdot\hat{S}_j$, where J is the exchange parameter. The spin Hamiltonian for model 1 is

$$\hat{H} = -2J_1[\hat{S}_1\cdot\hat{S}_2 + \hat{S}_1\cdot\hat{S}_3] - 2J_2\hat{S}_2\cdot\hat{S}_3 \tag{1}$$

The vector coupling method of Kambe[27] was used to obtain the eigenvalues, which are given by

$$\begin{aligned} E(S_T,S_A) &= -J_1[S_T(S_T + 1) - S_A(S_A + 1) - S_1(S_1 + 1)] \\ &\quad -J_2[S_A(S_A + 1) - S_2(S_2 + 1) - S_3(S_3 + 1)] \end{aligned} \tag{2}$$

The total spin is given as $S_T = S_1 + S_A$, where $S_A = S_2 + S_3$. There are four energy levels when $J_1 \neq J_2$. The paramagnetic susceptibility per mole of $Ni(phenSQ)_2(py)_2$ is given by

$$\begin{aligned} \chi_M = {} & [g^2\beta^2N/3k(T - \Theta)][30 \exp(x/kT) + \\ & 6 \exp(y/kT) + 6 \exp(z/kT)]/[5 \exp(x/kT) + \\ & 3 \exp(y/kT) + 3 \exp(z/kT) + \exp(w/kT)] \end{aligned} \tag{3}$$

where $S_1 = 1$ and $S_2 = S_3 = {}^1/_2$. In this expression the symbols have their usual meanings: Θ is the Curie–Weiss constant to gauge *inter*molecular interactions and the exponential terms are defined as

$$x = 2J_1 + \frac{J_2}{2} \qquad y = -2J_1 + \frac{J_2}{2} \qquad z = -\frac{3J_2}{2} \qquad w = -4J_1 + \frac{J_2}{2} \tag{4}$$

In theoretical model 2 for the magnetic susceptibility of $Ni(phenSQ)_2(py)_2$, it is assumed that the dominant magnetic exchange is associated with the pairwise phenSQ–phenSQ interaction, and this is gauged with the exchange parameter J_Q. A second parameter J_D is also used for the interaction between the metal ion and the nonstacked phenSQ ligand. The molar paramagnetic susceptibility is given for a dimer, e.g., $[Ni(phenSQ)_2(py)_2]_2$, and is simply evaluated as

$$\chi_M = \chi(\text{phenSQ–phenSQ}) + 2\chi(\text{Ni–phenSQ}) \tag{5}$$

where for the phenSQ pair

$$\chi(\text{phenSQ–phenSQ}) = \frac{g^2\beta^2N}{3k(T - \Theta)}\left[\frac{6 \exp(2J_Q/kT)}{1 + 3 \exp(2J_Q/kT)}\right] \tag{6}$$

The contribution for the Ni–phenSQ moiety is

$$\chi(\text{Ni–phenSQ}) = \frac{g^2\beta^2N}{3k(T - \Theta)}\left[\frac{3 + \exp(3J_D/kT)}{4 + \exp(3J_D/kT)}\right] \tag{7}$$

The magnetic susceptibility data for $Ni(phenSQ)_2(py)_2$ were least-squares fit to eq 3 and 5 resulting from models 1 and 2, respectively. The best fit to eq 3, which is the isolated $Ni(phenSQ)_2(py)_2$ model, gives $g = 2.25$, $J_1 = J_2 = 0.0$ cm^{-1}, and $\Theta = -6.5$ K. This fit is indicated by solid lines in Figure 3 (data as open circles). Thus, the shape of the χ vs. T curve at low temperatures is not in keeping with the equation for *intra*molecular interactions in $Ni(phenSQ)_2(py)_2$, but a negative Θ value is better. This is in keeping with the results of the X-ray structure which show a strong pairwise interaction of two $Ni(phenSQ)_2(py)_2$ complexes. Fitting the data to eq 5 gives $g_D = 2.35$, $g_A = 2.00$, $J_Q = -55$ cm^{-1}, $J_D = 0.0$ cm^{-1}, and $\Theta = 4.7$ K. This fit to eq 5 is also illustrated in Figure 3. In this case, the data are plotted with filled circles. It is clear, however, that most of the decrease in μ_{eff} at low temperature [at 4.2 K it is 2.62 μ_B per $Ni(phenSQ)_2(py)_2$ molecule] is due to the phenSQ–phenSQ interaction. This is substantiated by the data for $Ni(3,5\text{-}DBSQ)_2(bpy)$, which are given in Table VI[26] and in Figure 4. The *tert*-butyl substituents on the semiquinone ligands prevent *inter*molecular interactions. It can be seen that μ_{eff} per $Ni(3,5\text{-}DBSQ)_2(bpy)$ is relatively constant at ca. 4.3 μ_B at high temperature, with a relatively small decrease to 3.9 μ_B at 4.2 K. This small drop in μ_{eff} could be due to *intra*molecular interactions. Fitting the data for this complex to eq 3 gives $g = 2.33$, $J_1 = -0.7$ cm^{-1}, and $J_2 = 0.0$ cm^{-1} with Θ fixed at zero. The *intra*molecular magnetic exchange interactions between coordinated semiquinone and paramagnetic metal ion are indeed very weak in these two nickel(II) complexes.

Unfortunately only one "mononuclear" bis(semiquinone) cobalt complex was prepared and studied, $Co(phenSQ)_2(py)_2$. The complex $Co(3,5\text{-}DBSQ)(3,5\text{-}DBCat)(bpy)$ has one semiquinone and one hydroquinone dianion bonded to a low-spin cobalt(III) ion.[20] Figure 5 (Tables VI and VII[26]) gives the χ vs. T and μ_{eff} vs. T data for $Co(phenSQ)_2(py)_2$ plotted in two different ways. The filled-circle representation corre-

---

(27) Kambe, K. *J. Phys. Soc. Jpn.* **1950**, *5*, 48.

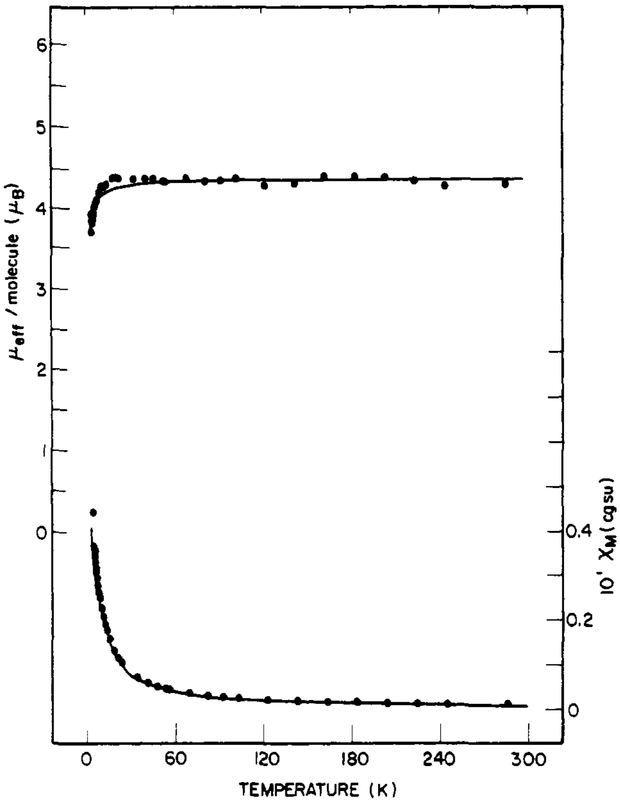

Figure 4. Effective magnetic moment *per molecule* and molar paramagnetic susceptibility *per molecule* vs. temperature curves for Ni(3,5-DBSQ)$_2$(bpy). The solid lines represent the fit to a theoretical model; see text.

sponds to model 1 for *intra*molecular interactions in isolated Co(phenSQ)$_2$(py)$_2$. In this case $S_1 = {}^3/_2$ and $S_2 = S_3 = {}^1/_2$; the susceptibility expression for the nickel case (eq 3) is modified to give for the paramagnetic susceptibility per mole of Co(phenSQ)$_2$(py)$_2$

$$\chi_M = [g^2\beta^2N/3k(T-\Theta)][52.5\exp(w/kT) + 30\exp(x/kT) + 1.5\exp(y/kT) + 30\exp(z/kT)]/[6\exp(w/kT) + 4\exp(x/kT) + 2\exp(y/kT) + 4\exp(z/kT)] \quad (8)$$

The exponential terms in this expression are defined as

$$w = 3J_1 + \frac{J_2}{2} \qquad x = -2J_1 + \frac{J_2}{2} \qquad y = -5J_1 + \frac{J_2}{2} \qquad z = \frac{-3J_2}{2} \quad (9)$$

Least-squares fitting the data for Co(phenSQ)$_2$(py)$_2$ to eq 7 gives $g = 2.47$, $J_1 = -3.6$ cm^{-1}, $J_2 = 0.0$ cm^{-1}, and $\Theta = -0.06$ K. Examination of Figure 5 shows that the fit to this model 1 is very reasonable; the maximum in the χ vs. T curve is fit well.

Theoretical model 2 was also modified to treat the Co(phenSQ)$_2$(py)$_2$ data. Open circles in Figure 5 are appropriate in this case. As before, the pairwise phenSQ-phenSQ association is emphasized. The term χ(Ni(phenSQ)) is replaced byχ(Co(phenSQ)) in eq 5, where the latter is given as

$$\chi(\text{Co(phenSQ)}) = \frac{g^2\beta^2N}{3k(T-\Theta)}\left[\frac{6 + 30\exp(4J_D/kT)}{3 + 5\exp(4J_D/kT)}\right] \quad (10)$$

Fitting to eq 9 gives $g_D = 2.50$, $g_Q = 2.00$, $J_Q = -5.7$ cm^{-1},

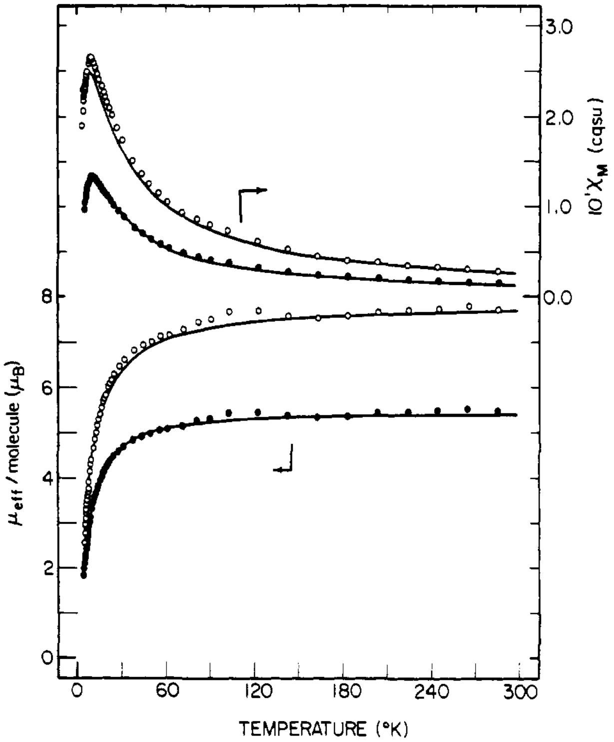

Figure 5. Effective magnetic moment and molar paramagnetic susceptibility vs. temperatures curves for Co(phenSQ)$_2$(py)$_2$. The data are plotted in two different ways. In one case (●) the μ_{eff} and χ_M values are given per Co(phenSQ)$_2$(py)$_2$ unit, whereas in the other case (○) the data are given per dimer [Co(phenSQ)$_2$(py)$_2$]$_2$. The solid lines represent least-squares fits to two different models; see text.

$J_D = -2.4$ cm^{-1}, and $\Theta = -11.3$ K. As can be seen in Figure 5, model 2 does not fit the maximum region in the χ vs. T curve as well as does model 1.

Magnetism of Tetranuclear Complexes. Variable-temperature magnetic susceptibility data were obtained for Co$_4$(3,5-DBSQ)$_8$, Co$_4$(phenSQ)$_8$, Ni$_4$(3,5-DBSQ)$_8$, and Ni$_4$(phenSQ)$_8$; the data are collected in Tables X–XIII.[26] Figure 6 shows the temperature dependence of μ_{eff} per tetranuclear complex as a function of temperature for these four complexes. It can be seen (see Table IX) that the two cobalt complexes have μ_{eff} values of ca. 9.2 μ_B at 244 K based on a tetranuclear formulation. The X-ray structure[18] of Co$_4$(3,5-DBSQ)$_8$ does show a complicated tetranuclear molecular composition where the tetranuclear complexes are fairly isolated in the solid state as a result of the *tert*-butyl groups on the eight semiquinone ligands. At this point it is assumed that the Co-phenSQ complex also has a tetranuclear composition. The room-temperature effective magnetic moments have also been measured for Co$_4$(3,5-DBSQ)$_8$ and Co$_4$(phenSQ)$_8$ as 9.50 and 9.34 μ_B (per tetranuclear complex), respectively.[18]

At the outset it must be admitted that developing a theoretical model to fit the susceptibility data for these tetranuclear complexes is a considerable challenge that we have only partially met. At the very least it is a simple matter to calculate the expected spin-only μ_{eff} for such a complex under the conditions where there is no magnetic exchange interaction between the $S = {}^3/_2$ cobalt(II) ions and the coordinated $S = {}^1/_2$ semiquinone ligands. The shortest Co–Co distance is 3.162 (2) Å,[18] and, as such, it can be safely assumed there is little Co–Co interaction. The spin-only value of μ_{eff} per tetranuclear complex is obtained by adding together the spin-only magnetic susceptibilities of four high-spin $S = {}^3/_2$ cobalt(II) ions and eight $S = {}^1/_2$ semiquinones. This gives a value of $\mu_{eff} = 9.16$ μ_B per Co$_4$(*o*-semiquinone)$_8$ or $\mu_{eff} = 4.58$ μ_B per Co(*o*-semiquinone)$_2$ moiety. It must be emphasized that only magnetic susceptibilities are additive, not effective magnetic

Table XIV. Least-Squares Fitting of Parameters for Tetranuclear M_4(*o*-semiquinone)$_8$ Complexes

	model 1				model 2					
compd	g	J_1, cm^{-1}	J_2, cm^{-1}	Θ, K	g_T	g_D	J_1, cm^{-1}	J_2, cm^{-1}	J_D, cm^{-1}	Θ, K
$Co_4(DBSQ)_8$	2.0	0.0	0.0	−14.7	2.5	2.5	−29.6	0.0	0.0	−5.3
$Co_4(phenSQ)_8$	2.0	0.0	0.0	−3.6	2.34	2.34	−3.5	0.0	0.0	0.0
$Ni_4(DBSQ)_8$	2.35	−0.5	0.0	−5.0						
$Ni_4(phenSQ)_8$					2.0	2.0	−6.1	0.0	0.0	−2.0

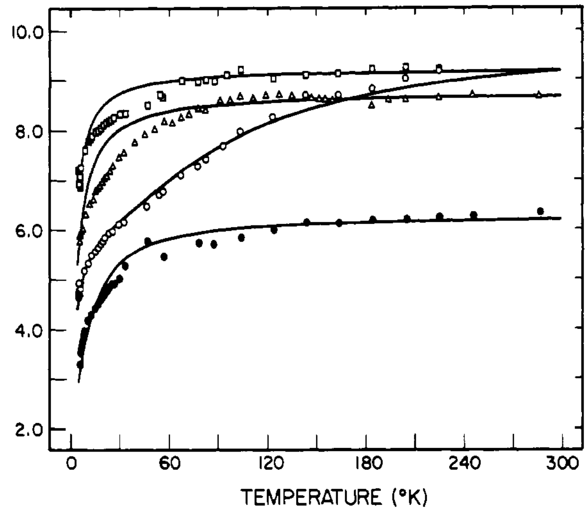

Figure 6. Effective magnetic moment *per tetranuclear complex* vs. temperature curves for $Co_4(phenSQ)_8$ (□), $Co_4(3,5\text{-}DBSQ)_8$ (○), $Ni_4(3,5\text{-}DBSQ)_8$ (△), and $Ni_4(phenSQ)_8$ (●).

moments. It is *not* correct to count unpaired electrons for a Co(*o*-semiquinone)$_2$ moiety and conclude that there will be a spin-only μ_{eff} appropriate for $S = {}^5/_2$ ($\mu_{eff} = 5.92\ \mu_B$). The experimental values of μ_{eff} for $Co_4(3,5\text{-}DBSQ)_8$ and $Co_4(phenSQ)_8$ are in excess of the spin-only μ_{eff} calculated for the case where there are no interactions between the semiquinone ligand unpaired electrons and the unpaired electrons of the cobalt(II) ions. There is only one conclusion that can be drawn from this observation, namely, that these tetranuclear cobalt complexes are, in fact, high-spin cobalt(II) complexes with semiquinone ligands and weak *intra*molecular magnetic exchange interactions.

Two simple theoretical models were used to fit the data for the two tetranuclear cobalt complexes. It would be expected that *inter*molecular magnetic exchange interactions would be weaker in $Co_4(3,5\text{-}DBSQ)_8$ than in $Co_4(phenSQ)_8$, because the former has *tert*-butyl substituents. It appears, then, that the magnitude of *intra*molecular antiferromagnetic exchange is greater in $Co_4(3,5\text{-}DBSQ)_8$. This is indicated by the fact that there is a greater decrease (reduced to 4.63 μ_B at 4.2 K) in μ_{eff} as the sample temperature is decreased for $Co_4(3,5\text{-}DBSQ)_8$ than for $Co_4(phenSQ)_8$ (see Figure 6).

A stereoscopic plot of $Co_4(3,5\text{-}DBSQ)_8$ is given in Figure 7, which, if studied for some period of time, shows that there are two *o*-semiquinone ligands that each chelate only one cobalt(II) ion. Each of the other six *o*-semiquinone ligands has one oxygen atom interacting with only one cobalt(II) ion; the other oxygen atom is bridging either two or three cobalt(II) ions. If we assume that interactions between semiquinone ligands and cobalt(II) ions are transmitted best by the nonbridging oxygen atoms and if we assume that magnetic exchange interactions are not propagated by Co–O–Co pathways, then the magnetic susceptibility of a Co$_4$(*o*-semiquinone)$_8$ complex is equal to the summation of 4 times the susceptibility of a Co(*o*-semiquinone)$_2$ unit. This is model 1 for the tetranuclear complexes. The parameters in this model are J_1 gauging the interaction between the cobalt(II) ion and a semiquinone in Co(*o*-semiquinone)$_2$, J_2 gauging the interaction between the two semiquinones, and a Curie–Weiss constant Θ. Table XIV lists the parameters obtained for the best least-squares fit of the data for $Co_4(3,5\text{-}DBSQ)_8$ and $Co_4(phenSQ)_8$ to model 1. The two fits are not very good; the fit to model 1 for the phenSQ complex is illustrated in Figure 6. The best fits were found for $J_1 = J_2 \simeq 0$ and with appreciable values of Θ: −3.6° (phenSQ) and −14.7° (3,5-DBSQ).

Theoretical model 2 for the tetranuclear complexes also makes the assumption that there are four isolated M(*o*-semiquinone)$_2$ units in the complex. It differs from model 1 in that it further assumes in the case of two of the four M(*o*-semiquinone)$_2$ that the unpaired electron for the *o*-semiquinone which is only chelating one cobalt(II) ion is effectively paired up with one of the metal electrons. Thus, the cobalt tetranuclear complex is assumed to be made up of two Co(*o*-semiquinone)$_2$ units and two $S_1' = 1$, $S_2 = {}^1/_2$ exchange interacting pairs. The exchange interaction in the $S_1' = 1$, $S_2 = {}^1/_2$ pair is gauged by the parameter J_D, where $S_2 = {}^1/_2$ is for the weakly interacting semiquinone, and $S_1' = 1$ results from the assumed strong coupling between the cobalt(II) ion and the chelated semiquinone. As in model 1, J_1 and J_2 are used to characterize the interaction in the two Co(*o*-semiquinone)$_2$ units. The least-squares fit of the data for $Co_4(3.5\text{-}DBSQ)_8$ to model 2 is shown in Figure 6. It can be seen in Table XIII that the large decrease in μ_{eff} with decreasing temperature for $Co_4(3,5\text{-}DBSQ)_8$ is handled by the parameter $J_1 = -30$ cm^{-1}, whereas $J_2 = J_D \simeq 0$.

It is clear that theoretical models 1 and 2 for the tetranuclear complexes are too simplified, and it is likely that there are interactions propagated by Co–O–Co pathways. Nevertheless, the two models do set upper limits to the magnitude of antiferromagnetic interaction between the cobalt(II) ions and coordinated semiquinone ligands.

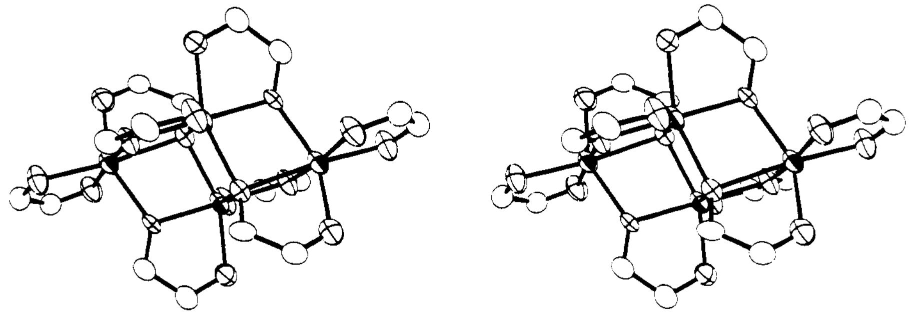

Figure 7. Stereoscopic ORTEP plot of $Co_4(3,5\text{-}DBSQ)_8$. Only two carbon atoms for each *o*-semiquinone ligand are shown for clarity.

There is an interesting and intriguing difference in the magnetic susceptibility characteristics of $Ni_4(3,5\text{-}DBSQ)_8$ and $Ni_4(phenSQ)_8$, as can be seen in Figure 6. The 3,5-DBSQ complex has a moment of 8.69 μ_B per tetranuclear complex at 286 K, whereas the phenSQ complex gives 6.32 μ_B at the same temperature. If there were no exchange interactions between any of the two nickel(II) ions and eight semiquinone ligands in these complexes, the spin-only μ_{eff} per tetranuclear complex would be 7.48 μ_B. The μ_{eff} value for $Ni_4(3,5\text{-}DBSQ)_8$ exceeds this value, which can only mean that there are semiquinone ligands and that the *intra*molecular magnetic exchange interactions are all weak. As per model 2, if it is assumed that there is a relatively strong interaction between each chelated semiquinone and its metal ion to give two $S = {}^1/_2$ nickel–semiquinone units and all other interactions are very weak, then the spin-only value of μ_{eff} per tetranuclear complex would be 6.32 μ_B. It is perhaps fortuitous that this is the μ_{eff} value obtained for $Ni_4(phenSQ)_8$ at 286 K. The least-squares fit of the data for this compound to theoretical model 2, furthermore, gives $J_1 = -6.1$ cm^{-1} for the nickel–semiquinone interaction in the two weakly coupled $Ni(phenSQ)_2$ units (see Table XIII). On the other hand, the data for $Ni_4(3,5\text{-}DBSQ)_8$ were only fit to theoretical model 1 to find $J_1 = -0.5$ cm^{-1}, $J_2 = 0.0$ cm^{-1}, and $\Theta = -5.0$ K.

Magnetism of Tris(semiquinone) Complexes. In a previous paper[14] we reported the magnetic susceptibility characteristics of three different tris(*o*-semiquinone) ferric complexes, as well as those of two different tris(*o*-semiquinone) complexes of chromium(III). The complex $Fe(3,5\text{-}DBSQ)_3$ behaves as a $S = 1$ complex with two unpaired electrons in the ground state; μ_{eff} is relatively independent of temperature with a value of 2.90 ± 0.05 μ_B. The other two iron(III) complexes have room-temperature μ_{eff} values that are in excess of this value and show pronounced temperature dependence, which is in keeping with the suggestion that the *intra*molecular antiferromagnetic exchange interaction between iron(III) and chelated *o*-semiquinone is of moderate strength, i.e., less than 400 cm^{-1}. Similar observations were made for the two chromium complexes. The theoretical susceptibility equations needed to determine at least the lower limit to the exchange parameters in these complexes were derived as traced out below.

In the case of the $M(o\text{-semiquinone})_3$ complexes there is but a single exchange parameter gauging the interaction of the metal ion with the paramagnetic ligand, and the spin Hamiltonian can be written as

$$\hat{H} = -2J[\hat{S}_1\cdot\hat{S}_2 + \hat{S}_1\cdot\hat{S}_3 + \hat{S}_1\cdot\hat{S}_4] \quad (11)$$

In this expression, $\hat{S}_1$ is the spin operator of the metal ion and $\hat{S}_2$, $\hat{S}_3$, and $\hat{S}_4$ are those for the three *o*-semiquinone ligands. The vector coupling method of Kambe[27] is used where the total spin is $S_T = S_1 + S_B$, and the coupling is done such that $S_B = S_A + S_4$, where $S_A = S_2 + S_3$. With this approach the eigenvalues are found to be

$$E(S_T) = -J[S_T(S_T + 1) - S_1(S_1 + 1) - S_B(S_B + 1)] \quad (12)$$

For a $Fe^{III}(o\text{-semiquinone})_3$ complex, $S_1 = {}^5/_2$ and $S_2 = S_3 = S_4 = {}^1/_2$, which leads to eq 13 for the molar paramagnetic

$$\chi_M = [g^2\beta^2N/3kT][180 + 84 \exp(a/kT) + 30 \exp(b/kT) + 6 \exp(c/kT) + 168 \exp(d/kT) + 60 \exp(e/kT)]/[9 + 7 \exp(a/kT) + 5 \exp(b/kT) + 3 \exp(c/kT) + 14 \exp(d/kT) + 10 \exp(e/kT)] \quad (13)$$

susceptibility per tris(*o*-semiquinone) complex. The exponential terms in the above expression are $a = 8J$, $b = 14J$, $c = 18J$, $d = 5J$, and $e = 11J$. In the case of the $Cr^{III}(o\text{-semiquinone})_3$ complexes, $S_1 = {}^3/_2$ and $S_2 = S_3 = S_4 = {}^1/_2$ to give eq 14. In this equation $a = 6J$, $b = 10J$, $c = 12J$, $d = 3J$, and $e = 7J$.

$$\chi_M = [g^2\beta^2N/3kT] \times [84 + 30 \exp(a/kT) + 6 \exp(b/kT) + 60 \exp(d/kT) + 12 \exp(e/kT)]/[7 + 5 \exp(a/kT) + 3 \exp(b/kT) + \exp(c/kT) + 10 \exp(d/kT) + 6 \exp(e/kT)] \quad (14)$$

Table XV. Magnetic Exchange Parameters for Metal-Semiquinone Complexes

compd[a]	$-J$, cm^{-1} [b]	ref
One Semiquinone Ligand per Metal		
$Fe(salen)(3,5\text{-}DBSQ)$	⩾200	10
$Fe(salen)(1,2\text{-}NSQ)$[c]	⩾200	10
$Fe(salen)(phenSQ)$	⩾200	10
$Mn(salen)(3,5\text{-}DBSQ)$	⩾275	10
Two Semiquinone Ligands per Metal		
$Co(phenSQ)_2(py)_2$	3.6	*d*
$Ni(phenSQ)_2(py)_2$	ca. 0.0	*d*
$Ni(3,5\text{-}DBSQ)_2(bpy)$	0.7	*d*
$Co_4(3,5\text{-}DBSQ)_8$	ca. 30	*d*
$Co_4(phenSQ)_8$	ca. 0.0	*d*
$Ni_4(3,5\text{-}DBSQ)_8$	ca. 6.0	*d*
$Ni_4(phenSQ)_8$	*e*	*d*
Three Semiquinone Ligands per Metal		
$Fe(3,5\text{-}DBSQ)_3$	190	*f*
$Fe(o\text{-}Cl_4SQ)_3$[g]	60	*f*
$Fe(phenSQ)_3$	100	*f*
$Cr(phenSQ)_3$	350	*f*
$Cr(o\text{-}Cl_4SQ)_3$	400	*f*

[a] salen is the dianion of *N,N'*-ethylenebis(salicylidenimine). [b] Each metal–semiquinone interaction is characterized by a magnetic exchange parameter J as given in spin Hamiltonian $\hat{H} = -2J\hat{S}_1\cdot\hat{S}_2$. [c] 1,2-NSQ is the semiquinone of 1,2-naphthoquinone. [d] This work. [e] See text for discussion of this J value. [f] The magnetic susceptibility data are given in ref 14, while the analysis to determine the J value is carried out in this work. [g] *o*-Cl_4SQ is the semiquinone of *o*-chloranil.

The magnetic susceptibility data for the five tris(*o*-semiquinone) complexes were fit to the above equations to evaluate the exchange parameters. In some cases, e.g., $Fe(phenSQ)_3$, only the data above ca. 200 K were fit because the low-temperature data are probably affected by *inter*molecular interactions. In all cases it is only possible to find a lower limit for $-J$. Table XIV summarizes the results.

Intramolecular Magnetic Exchange as a Function of Metal Ion. It is clear from the present study that the *intra*molecular antiferromagnetic exchange interactions in metal–semiquinone complexes can range from moderately strong to quite weak. In Table XV are collected the estimates of exchange parameters for a variety of such complexes.

The *intra*molecular antiferromagnetic exchange interaction between coordinated *o*-semiquinone ligand and metal ion is strongest in the case of the tris(*o*-semiquinone) complexes of chromium(III) and high-spin iron(III) and the $Fe^{III}(salen)(o\text{-semiquinone})$ complexes. In all of these complexes, the magnitude of the exchange interaction is such that for a given sample at room temperature most of the molecules are in the ground state where there is the least paramagnetism. In the case of the tris(*o*-semiquinone) complexes of chromium(III) the ground state has $S = 0$ and the complexes are close to being diamagnetic (temperature-independent paramagnetism notwithstanding). On the other hand, very weak *intra*molecular exchange interactions are present in the nickel(II) and cobalt(II) complexes.

The order of decreasing *intra*molecular antiferromagnetic exchange interaction in the above *o*-semiquinone complexes is Cr(III) > Fe(III) > Co(II) > Ni(II). This order can be simply rationalized in terms of the molecular orbitals that are involved. Molecular orbital calculations on *o*-semiquinones show that the single unpaired electron resides in a π molecular orbital.[28] The metal e_g d orbitals in these pseudooctahedral complexes are, of course, σ antibonding orbitals, while the metal t_{2g} d orbitals are of the π type. It follows, then, that the chromium(III)–*o*-semiquinone complexes would be expected to exhibit the largest magnitude of antiferromagnetic exchange interaction, because the chromium(III) complexes are d^3 complexes where all of the unpaired d electrons are in t_{2g} orbitals and can interact very effectively with the unpaired electrons of the *o*-semiquinone ligands. In the case of the high-spin iron(III) complexes, there are also three unpaired t_{2g} electrons to effect an appreciable *net* antiferromagnetic interaction, but the *net* antiferromagnetic interaction is probably reduced by virtue of the presence of ferromagnetic exchange pathways between the unpaired electrons of the *o*-semiquinone ligands and the unpaired electrons of the metal. The latter are the consequence of the presence of two unpaired e_g metal electrons in the case of the high-spin iron(III) complexes. The net antiferromagnetic interaction is quite weak for the cobalt(II) and nickel(II) complexes, because they have more unpaired electrons in e_g d orbitals than in t_{2g} d orbitals.

Acknowledgment. D.N.H. is grateful for funding from National Institutes of Health Grant HL13652 and Biomedical Research Grant RR 07030. Research at the University of Colorado is supported by National Institutes of Health Grant GM 23386 and by funds from American Cyanamid.

Registry No. $Ni(phenSQ)_2(py)_2{\cdot}py$, 76136-01-1; $Co(phenSQ)_2(py)_2$, 76136-02-2; $Ni(3,5\text{-}DBSQ)_2(bpy)$, 76136-03-3; $Co_4(3,5\text{-}DBSQ)_8$, 71370-70-2; $Co_4(phenSQ)_8$, 76172-93-5; $Ni_4(3,5\text{-}DBSQ)_8$, 76190-17-5; $Ni_4(phenSQ)_8$, 76137-18-3; $Fe(3,5\text{-}DBSQ)_3$, 70755-84-9; Fe(*o*-$Cl_4SQ)_3$, 67291-91-2; $Fe(phenSQ)_3$, 39797-84-7; $Cr(phenSQ)_3$, 68846-34-4; Cr(*o*-$Cl_4SQ)_3$, 60635-34-9.

Supplementary Material Available: Tables IV–VIII and X–XIII (calculated and observed magnetic susceptibility data) and listings of observed and calculated structure factors (23 pages). Ordering information is given on any current masthead page.

---

(28) (a) Pilar, J. *J. Phys. Chem.* **1970**, *74*, 4029. (b) Kuwata, K.; Shimizu, Y. *Bull. Chem. Soc. Jpn.* **1969**, *42*, 864. (c) Broze, M.; Luz, Z. *J. Chem. Phys.* **1969**, *51*, 738. (d) Pasimeni, L.; Brustolon, J.; Corvaja, C. *Chem. Phys. Lett.* **1975**, *30*, 249.

Contribution from University Chemical Laboratories,
Cambridge CB2 1EW, England

Donor and Acceptor Properties of Triphenylphosphine Ligands in Trigonally Distorted Tetrahedral $NiPX_3^-$ Chromophores (X = Br, I)

MALCOLM GERLOCH* and LYALL R. HANTON

Received July 28, 1980

Single-crystal paramagnetic susceptibilities are reported for $[Ph_4As]^+[Ni(PPh_3)Br_3]^-$ throughout the temperature range 20–30 K and powder susceptibilities in the range 70–300 K for $[Ph_4As]^+[Ni(PPh_3)I_3]^-$. These and the published crystal transmission spectra are analysed within the angular overlap model. Optimized parameter sets describe strong σ basicity and strong π acidity of the phosphine ligands, the magnitudes of which change somewhat in response to the differing basicity of the bromine and iodine ligands. Very small spin–orbit coupling coefficients are observed in these complexes and, in comparison with values in other systems, identify a common feature of tetrahedrally coordinated nickel(II) complexes.

Introduction

The characterization of the individual roles of σ- and π-ligand coordination in transition-metal complexes is a principal aim of current studies of spectroscopic and magnetic properties within the framework of the angular overlap model.[1] A recent analysis[2] of the single-crystal paramagnetism and optical spectra of the phosphine complexes $M(PPh_3)_2X_2$ [M = Ni(II), Co(II); X = Cl, Br] has provided a semiquantitative demonstration of considerable π acidity of the coordinated phosphine groups associated with a enhanced π basicity of the halogens. A phosphine π-acceptor role was similarly identified[3] in the low-spin, planar complex dimesitylbis(diethylphenylphosphine)cobalt(II).

The present study concerns the complexes $[Ph_4As]^+[Ni(PPh_3)X_3]^-$ (X = Br, I) which provide opportunities for comparison between (a) mono and bis coordinated phosphine complexes in "tetrahedral" nickel(II) systems, (b) bromo and iodo ligand field parameters, and (c) trigonal and tetragonal distortions in these tetrahedral chromophores. Single-crystal spectroscopic and paramagnetic properties of these compounds are reproduced within our model virtually uniquely by parameters which establish a number of interesting features: (i) The phosphine ligands act as relatively strong Lewis bases via σ bonding with the central nickel(II) ion and, at the same time, as substantial Lewis acids via π bonding. These properties are somewhat enhanced in the iodo complex with respect to the bromo one. (ii) The π-donor function is greater for the bromine ligands than for the iodines but less than observed[2] in the bis(phosphine) complexes $M(PPh_3)_2X_2$ (X = Cl, Br). (iii) The σ-donor property of the iodine ligands is less than that of the bromines which is much less than that of the phosphines. (iv) The magnetic susceptibilities of these complexes are only reproduced with a very low value for the spin–orbit coupling coefficient. This circumstance, which appears to be a common feature of tetrahedral nickel(II) systems, may reflect a participation[4] of halogen orbitals within the ground state and/or a significant role for dynamic Jahn–Teller coupling within the Ham effect.[5]

Experimental Section

The complexes $[Ph_4As]^+[Ni(PPh_3)X_3]^-$ (X = Br, I) were prepared as described in the literature.[6,7] Crystals of the bromo complex grown

---

(1) M. Gerloch, *Prog. Inorg. Chem.*, **26**, 1 (1979).

(2) J. E. Davies, M. Gerloch, and D. J. Phillips, *J. Chem. Soc. Dalton Trans.*, 1836 (1979).

(3) L. R. Falvello and M. Gerloch, *Inorg. Chem.*, **19**, 472 (1980).

(4) J. E. Collingwood, P. Day, and R. G. Denning, *J. Chem. Soc., Faraday Trans. 2*, **69** (4), 591 (1973).

(5) F. S. Ham, *Phys. Rev. A*, **138**, 1727 (1965).